Traffic 2003; 4: 273–288
Blackwell Munksgaard

ISSN 1398-9219

Differential Distribution of Low-Density Lipoprotein-Receptor-Related Protein (LRP) and Megalin in Polarized Epithelial Cells is Determined by Their Cytoplasmic Domains

María-Paz Marzolo[1,*], María Isabel Yuseff[1,2], Claudio Retamal[1], Maribel Donoso[1], Fernando Ezquer[2], Pamela Farfán[1], Yonghe Li[3] and Guojun Bu[3]

[1] Centro de Regulación Celular y Patología, Departamento de Biología Celular y Molecular, Facultad de Ciencias Biológicas, Pontificia Universidad Católica de Chile, Santiago, Chile
[2] Departamento de Biología, Facultad de Ciencias, Universidad de Chile, Santiago, Chile
[3] Department of Pediatrics, Washington University School of Medicine, St Louis, MO 63110, USA
* Corresponding author: María-Paz Marzolo, mmarzolo@bio.puc.cl

Received 11 November 2002, revised and accepted for publication 20 January 2003

Megalin and the low-density lipoprotein (LDL) receptor-related protein (LRP) are two large members of the LDL receptor family that bind and endocytose multiple ligands. The molecular and cellular determinants that dictate the sorting behavior of these receptors in polarized epithelial cells are largely unknown. Megalin is found apically distributed, whereas the limited information on LRP indicates its polarity. We show here that in Madin-Darby canine kidney cells, both endogenous LRP and a mini-receptor containing the fourth ligand-binding, transmembrane and LRP cytosolic domains were basolaterally sorted. In contrast, minireceptors that either lacked the cytoplasmic domain or had the tyrosine in the NPTY motif mutated to alanine showed a preferential apical distribution. In LLC-PK1 cells, endogenous megalin was found exclusively in the apical membrane. Studies were also done using chimeric proteins harboring the cytosolic tail of megalin, one with the fourth ligand-binding domain of LRP and the other two containing the green fluorescent protein as the ectodomain and transmembrane domains of either megalin or LRP. Findings from these experiments showed that the cytosolic domain of megalin is sufficient for apical sorting, and that the megalin transmembrane domain promotes association with lipid rafts. In conclusion, we show that LRP and megalin both contain sorting information in their cytosolic domains that directs opposite polarity, basolateral for LRP and apical for megalin. Additionally, we show that the NPTY motif in LRP is important for basolateral sorting and the megalin transmembrane domain directs association with lipid rafts.

Key words: apical, basolateral, green fluorescent protein, lipid rafts, LRP, megalin, polarized sorting

The low-density lipoprotein (LDL) receptor gene family contains three very large members, LRP (LRP1), a dimer of 515 kDa and 85 kDa, its closely related homolog, megalin (LRP2), a single species of ~600 kDa (1) and the recently discovered LRP1B, more closely related to LRP than to megalin (2). Comparison of LRP and megalin reveals that the overall protein domain structural organization of the two proteins is very similar. LRP has four ligand-binding domains (I, II, III, and IV from the N-terminus) separated from one another by clusters of EGF-precursor repeats and F/YWXD spacer repeats. LRP contains a furin endopeptidase processing site in its ectodomain that is cleaved to form the mature receptor, a noncovalently associated heterodimer, consisting of an extracellular 515-kDa subunit and a transmembrane 85-kDa subunit (3, 4). The cytoplasmic tail of LRP has 100 amino acids and harbors two NPxY motifs, one Yxxϕ motif, recently shown as the dominant endocytosis motif (5), and two LL motifs, with the distal one playing a small role in LRP internalization. In addition to these motifs, phosphorylation of the LRP tail by PKA also plays a role in the internalization of the receptor (6). Megalin contains four clusters of ligand-binding domains. The first ligand-binding domain is the most different from the corresponding domain in LRP, with seven ligand binding repeats instead of two (7). The transmembrane domain is followed by a 209 amino acid cytosolic tail with putative endocytosis motifs based on tyrosine and dileucine, a proline-rich sequence with homology to a SH3 binding domain, a carboxyl terminal PDZ motif and several putative phosphorylation motifs.

The LRP gene is essential for early embryonic development (8, 9). The receptor plays important roles in lipoprotein catabolism, blood coagulation, cell adhesion and migration, neuronal process outgrowth and the pathogenesis of Alzheimer's disease (1, 7, 10). The role LRP plays in these diverse biological processes is mediated by interactions with multiple ligands, including proteinases, proteinase-inhibitor complexes, and lipoprotein particles (7). LRP is also involved in signal transduction (11–13). The close similarity in protein domain structure between LRP and megalin explains their similarity in ligand

interaction, i.e. many LRP ligands may also be ligands for megalin. However, *in vivo* the overall biological function of megalin is different from that of LRP (14), and this explains in part the failure of megalin to rescue the lethality of an LRP knock-out. Megalin knock-out mice have severe forebrain abnormalities as well as lung defects, and most of them die perinatally (15), illustrating an important role for megalin in development (16). *In vivo* megalin is also important for the absorption of molecules by the intestine, reabsorption by the kidney and transport across the blood–brain barrier (7, 14). Megalin is expressed primarily in the apical domain of epithelial cells, while LRP is expressed broadly, both in epithelial and nonepithelial cells. In polarized cells such as neurons, LRP is localized in the somatodendritic domain (17), and in the liver LRP is localized in the sinusoidal face of the hepatocyte (18). Even if LRP and megalin were expressed in the same epithelial cells, they would probably be located in opposite plasma membrane domains, and thus each receptor would be exposed to a different set of ligands.

The plasma membrane of specialized cells such as neurons and epithelial cells is divided into functionally and morphologically distinct domains with different protein and lipid composition (19). In neurons the plasma membrane is composed of somatodendritic and axolemmal domains, whereas epithelial cells contain basolateral and apical domains. The different protein composition is maintained by several mechanisms, including protein sorting, from the *trans*-Golgi network (TGN) and endosomes to target membranes and selective retention in the plasma membrane (20). Many of these mechanisms rely upon protein–protein interactions directed by signals present within the targeted proteins themselves (21). Basolateral signals such as dihydrophobic repeats (LL; IL), tyrosine-containing sequences and other motifs that form tight β-turns are found in the cytosolic tail of many membrane proteins. Apical sorting can be mediated by different types of determinants, including signals in the lumenal domain as well as transmembrane domain and glycosylphosphatidylinositol anchors (22–24) that direct the protein to lipid rafts (23, 25, 26). It has been suggested that *N*-glycosylation is an apical determinant, but this is likely to be a relatively weak signal when a basolateral signal is coexpressed in the same protein (27), and is nonfunctional in some apical proteins (28). Other apical sorting determinants have been described in the cytoplasmic domains of some polytopic apical membrane proteins, such as rhodopsin (29), the amiloride-sensitive sodium channel (30) and cystic fibrosis transmembrane regulator (CFTR) (31). It has been proposed that in neurons the sorting behavior of some membrane proteins is equivalent to those found in epithelial cells. Apical proteins such as hemagglutinin (HA) and the majority of GPI anchored proteins are localized in the axon when expressed in neurons (32). Similarly, some axonal proteins are apical when expressed in the epithelial cell line MDCK (Madin-Darby canine kidney cells) (33). The transferrin receptor, basolateral in epithelial cells, is distributed on the dendritic surface in neurons (34).

In this study, we analyzed the localization of endogenous LRP and megalin and transfected chimeric proteins containing the tail of either megalin or LRP in epithelial polarized cell lines. We found that LRP contains sorting information located in the cytoplasmic domain, which allows the direct targeting of the minireceptor to the basolateral plasma membrane. Our results indicate that a tyrosine-based motif could have a role in the basolateral localization of the receptor. We also found that megalin and chimeric proteins containing the megalin tail are apically localized. Although the transmembrane region of megalin seems to have properties that permit it to associate with lipid rafts, this domain was not necessary for apical distribution. Instead, our results indicate that the cytosolic tail of megalin conveys apical information independently of raft association.

Results

Polarized expression of LRP and megalin in epithelial cells

The pig cell line LLC-PK1 is derived from kidney proximal tubule and forms a polarized monolayer when grown on filters. We found that both megalin and LRP are expressed in this cell line. By cell surface biotinylation, megalin was found to be apical (Figure 1A), as already described in epithelial tissues, and LRP showed a nonpolarized distribution (Figure 1B).

LLC-PK1 cells do not express the AP-1 subunit μ1b (35), which has been suggested to function in the basolateral sorting of membrane proteins with tyrosine-based signals, such as the LDL-R (36). In transfected LLC-PK1 cells expressing the AP1 subunit μ1B, LRP was instead distributed basolaterally (Figure 2A), indicating that it probably contains tyrosine-based motifs recognized by this adaptor protein. We next explored the expression and distribution

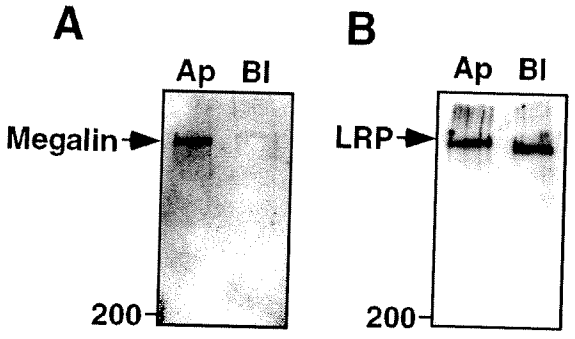

Figure 1: Distribution of LRP and megalin in polarized wild-type LLC-PK1 cells. LLC-PK1 cells were grown on filters for 5 days and biotinylated at either the apical domain (Ap) or the basolateral domain (Bl) at 4 °C. Following biotinylation, lysates were precipitated with streptavidin-Sepharose, separated by 5% SDS-PAGE and probed with anti-human megalin (A) or anti-human LRP (B).

of LRP in MDCK cells, which endogenously express μ1B (35) and correctly sort tyrosine-based membrane proteins to the basolateral membrane (36). In these cells, both by cell surface biotinylation (Figure 2B) and confocal microscopy (Figure 2C), LRP was basolaterally distributed. These results confirm that LRP has basolateral sorting information that requires the cell expression of the epithelial specific adaptor complex AP-1B to be deciphered correctly. As shown in Figure 3(A), the cytoplasmic domain of LRP has several basolateral putative motifs that could participate either in the direct basolateral targeting from the TGN and/or in the receptor recycling, in a postendocytic

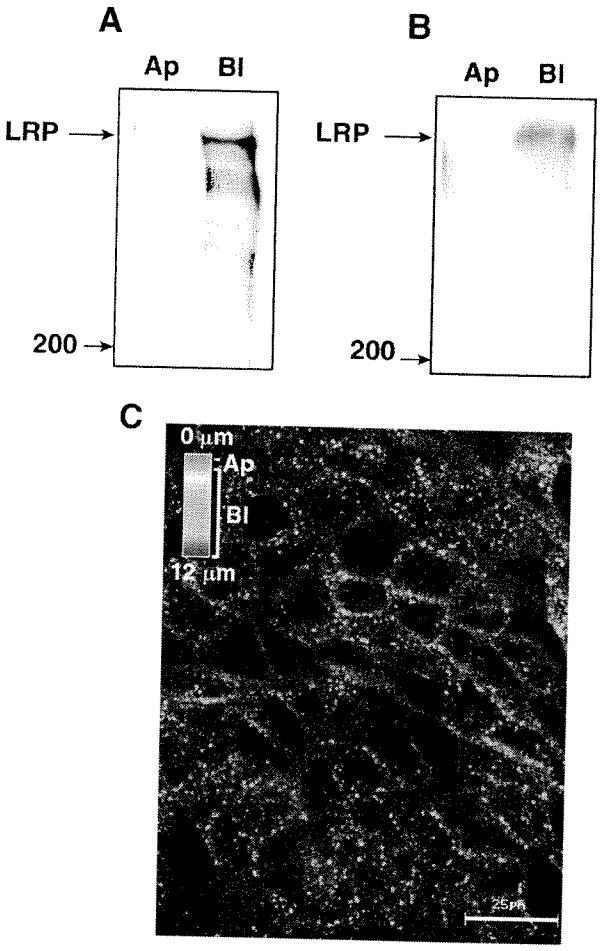

Figure 2: Basolateral expression of endogenous LRP in MDCK and LLC-PK1- μ1b cells. Filter-grown LLC-PK1-μ1b (A) and MDCK (B) cells were biotinylated either at the apical domain (Ap) or basolateral domain (Bl) at 4 °C. Following biotinylation, lysates were immunoprecipitated with anti-human LRP separated by 5% SDS-PAGE and probed with streptavidin-HRP. (C) MDCK cells grown on glass coverslips for 5 days until confluence were fixed and permeabilized with Triton-X100 and then successively incubated with anti-human LRP (1 : 100) and Cy3 conjugated anti-rabbit IgG. The sample was analyzed with a confocal microscope. An integration of all xy serial optical sections of 0.6-μm each is shown with an assigned color ranging from blue for basal to red for apical staining.

sorting event. There are tyrosine-based motifs, similar to the signals present in LDL-R (37) and also two dileucine motifs, that are functionally basolateral sorting signals as well (38, 39).

Construction of minireceptors with LRP and megalin cytoplasmic domains

Our working hypothesis was that the sorting information of LRP and megalin could be in their cytosolic tails. In Figure 3(A), the sequences of LRP, megalin, and LDL-R tails are shown for comparison. Several motifs that fit the described basolateral sorting signals of other proteins, including the LDL-R, are seen in both the LRP and megalin. The very large size of LRP and megalin (~600 kDa) limits the molecular manipulations at the cDNA level and the expression of this protein via transfection. Thus, we have generated LRP and megalin minireceptors to identify and characterize functional elements within the LRP and megalin tails determining the trafficking behavior of the receptors in polarized epithelial cells (Figure 3B). The LRP minireceptors consist of the fourth ligand-binding ectodomain followed by the transmembrane domain and either the complete cytosolic tail of LRP (mLRP/LRPTmT) or the complete 209 amino acids of the megalin tail (mLRP/LRPTmMegT). Two chimeric membrane proteins containing the GFP as ectodomain followed by either the transmembrane domain of LRP (GFP/LRPTmMegT) or megalin (GFP/MegTmT) and sharing the cytosolic domain of megalin were made. As controls for the sorting information that might be contained within the ectodomains and transmembrane domains of LRP, we made both a tailless minireceptor mLRP/LRPTmΔT and soluble forms of the minireceptor (SmLRP) and GFP (GFPsec). An HA epitope was inserted near the amino terminus of all the constructs to facilitate immunological detection of the minireceptor protein in transfected cells.

The cytosolic tail of LRP contains information for direct basolateral targeting

We decided to investigate whether a minireceptor containing the cytoplasmic domain of LRP behaves as the endogenous receptor in transfected MDCK cells. The total lysates of MDCK-mLRP/LRPTmT cells were analyzed by Western blot with anti-HA antibody. Both the precursor form of the minireceptor of 205 kDa and the mature form (furin processed) of 120 kDa were detected. Filter-grown MDCK cells expressing mLRP/LRPTmT were biotinylated to localize the steady-state cell surface minireceptor, which was found exclusively in the basolateral domain and in its processed form (Figure 4A, upper part). More than 95% of the receptor was localized in the basolateral domain of MDCK cells (average of several experiments, not shown). Biotinylated cells were correctly polarized, as shown by the apical distribution of an endogenous apical marker, gp135 (Figure 4A, bottom part). We confirmed the basolateral distribution of mLRP/LRPTmT by indirect immunofluorescence of permeabilized cells with anti-HA

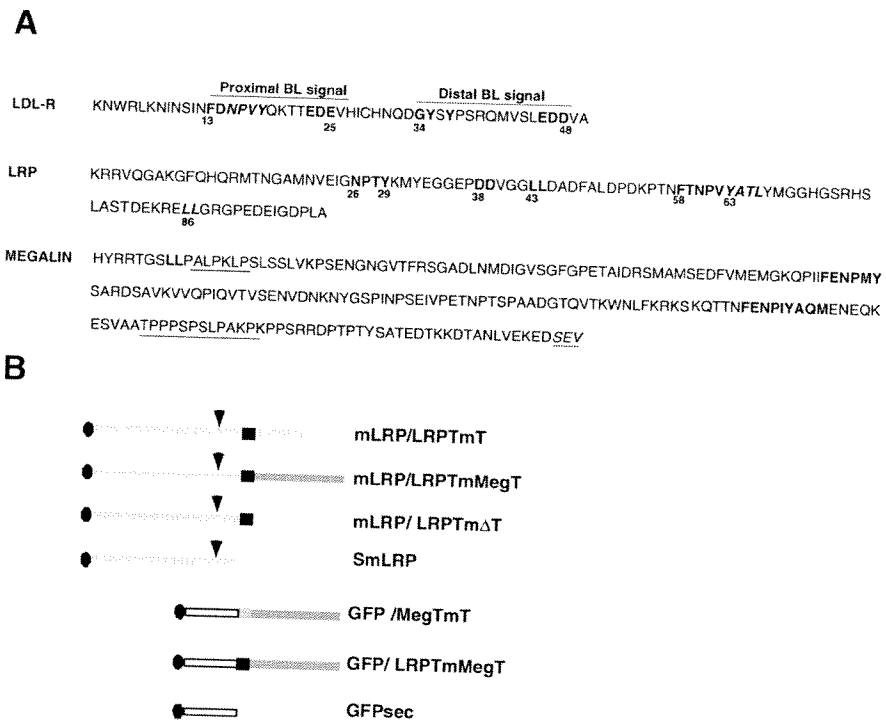

Figure 3: Sequence of the receptor tails and schematic representation of the LRP, megalin and GFP constructs. (A) Sequences of LDL-R, LRP and megalin tails showing the basolateral sorting motifs for LDL-R (67) and the putative basolateral motifs based on tyrosine and LL (bolded) present in the LRP tail. For LDL-R and LRP the known endocytosis motifs are also highlighted (bold italics) (5, 38). Within the megalin cytoplasmic domain sequence there are dileucine and tyrosine-based motifs (bolded), proline-rich sequences of the type of SH3-binding sites (underlined) and a carboxy terminal PDZ motif, SEV (italics, underlined). (B) The minireceptors, both membrane-bound (mLRP) and the soluble form (SmLRP), contain the fourth ligand-binding domain of LRP with the furin cleavage site (arrowhead) and the juxtamembrane domain of LRP. Additionally, the membrane-bound minireceptors contain the transmembrane domain of LRP (black box), either with no cytosolic domain, the cytosolic domain of LRP, or the cytosolic domain of megalin. The GFP/MegTmT chimera is made of GFP in the ectodomain, the megalin transmembrane domain and the cytoplasmic domain of megalin, whereas GFP/LRPTmMegT has the transmembrane region of LRP followed by the cytosolic domain of megalin. GFPsec is a secretable form of GFP. All the constructs were made with the HA epitope in the N-terminus (black oval).

antibody (Figure 4B). Both the endogenous LRP (see Figure 2C) and the minireceptor also gave an intracellular punctuate staining, probably corresponding to the recycling pathway. Because endogenous LRP is basolateral in cells expressing the AP-1B adaptor complex (Figure 2), but is nonpolarized in wild-type LLC-PK1 cells (Figure 1B), we investigated the participation of tyrosine-based motifs present in the receptor's tail. Using the mLRP/LRPTmT as a template, we made alanine site-directed mutagenesis in the first tyrosine (Y29A) belonging to a NPTY motif and in the second tyrosine (Y63A) that is part of two different and overlapping motifs, the NPVY and the YATL (see Figure 3A). The resulting mutated plasmids (mLRP/LRPTmT Y29A and mLRP/LRPTmT Y63A) were used to obtain stably transfected MDCK cell lines and study the localization of the minireceptors. As in shown in Figure 4(C), both by surface biotinylation and indirect immunofluorescence, the steady-state localization of the Y29A was apical, suggesting that the first NPxY motif is involved in the basolateral distribution on the receptor. Instead, the mutant of the tyrosine in position 63 also lost its polarity but appeared randomly distributed in the apical and basolateral domains. These results indicate that Y29 and Y63 contribute to the basolateral sorting, possibly with different strengths or through different mechanisms.

To determine if the basolateral localization of the minireceptor is only due to its cytosolic domain, it was necessary to show that the other domains of the protein have a neutral or distinct sorting behavior, in the same cell line. We then generated stable MDCK cell lines expressing the soluble form of the minireceptor (SmLRP) and the minireceptor mLRP/LRPTmΔT and analyzed their polarized expression in filter-grown cells. For SmLRP, cells were metabolically labeled with [^{35}S]methionine/cysteine for 60 min and chased for 4 h. After the chase, immunoprecipitations with anti-HA antibody were made from the apical and basolateral media and analyzed via SDS-polyacrylamide gel electrophoresis. As seen in Figure 5(A), the soluble forms of the minireceptor were processed by furin and secreted with a clear apical preference. The distribution of mLRP/LRPTmΔT was analyzed by indirect immunofluorescence anti-HA

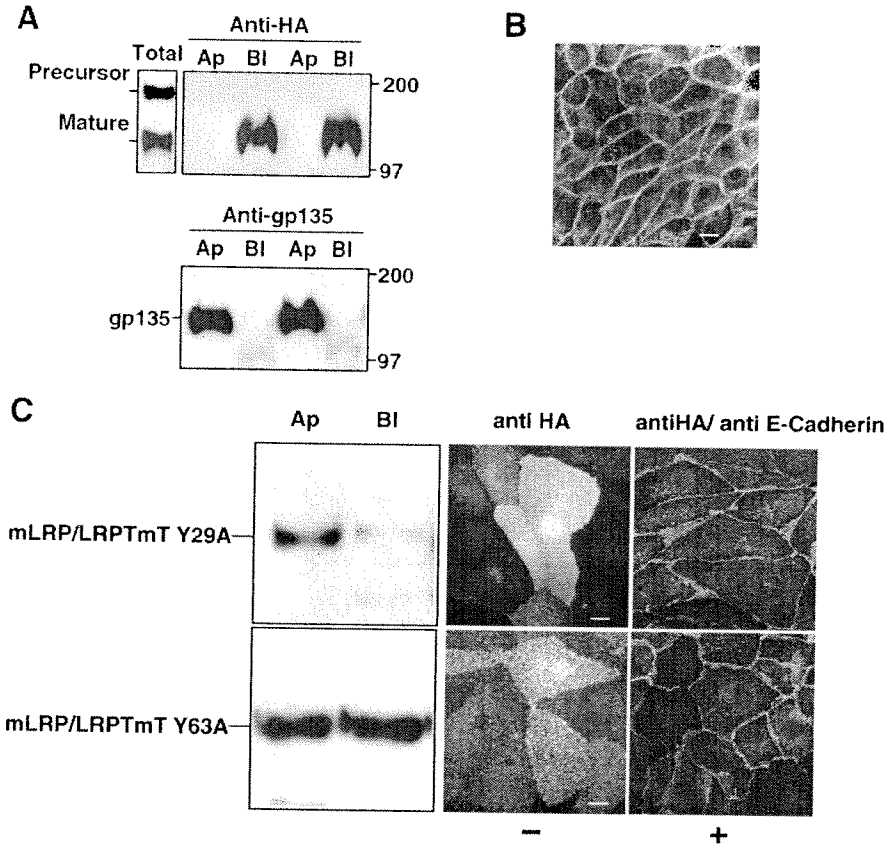

Figure 4: Distribution of the minireceptors with wild-type and tyrosine mutant LRP tails in MDCK cells. (A) Permanent transfectants of MDCK cells forming impermeable monolayers in Transwell chambers were analyzed for the polarized expression of mLRP/LRPTmT. Cells were selectively biotinylated in duplicate and the cell lysates treated as described in Experimental Procedures. A clear basolateral expression of the minireceptor is shown. Almost all the protein on the surface is the mature form, compared to the total lysate where the precursor form is also found. As a control of cell polarization and integrity of the cell apical pathway, the membrane was stripped and incubated with an antibody to detect the endogenous apical membrane protein, gp135. (B) mLRP/LRPTmT-expressing MDCK cells grown on coverslips were fixed, permeabilized and incubated with anti-HA. After incubation with the secondary antibody (anti-mouse IgG conjugated with FITC), cells were mounted and analyzed for immunofluorescence staining. The minireceptor is mainly restricted to the basolateral surface and to recycling vesicles. (C) MDCK cells expressing the Y29A and the Y63A minireceptors were grown on filters to perform selective biotinylation, showing that both tyrosines are important for the basolateral localization (left). Cells grown on glass coverslips were fixed and incubated with anti-HA (− non-permeabilized) or anti-HA plus anti E-Cadherin (+ permeabilized). Both mutants are expressed in the apical surface when they are visualized by indirect immunofluorescence (middle part of the figure). Permeabilized cells were analyzed by confocal microscopy to see the distribution of the mutant minireceptor and the colocalization with a basolateral marker, E-Cadherin. A basal-medial plane is shown to highlight that only the Y63A mutant has a basal localization as it can be colocalized with E-Cadherin (right part of the Figure) (scale bar, 10 μm).

on both sides of the filter. As is illustrated in Figure 5(B), this minireceptor also had a predominant apical distribution. A similar result was obtained by domain selective biotinylation (not shown). One possibility to explain the apical localization of the soluble and tailless minireceptors is the existence of apical sorting information in the ectodomain. The ectodomain of several basolateral proteins is believed to contain recessive information for apical localization that in some cases is dependent on *N*-glycosylation (19, 27). Because the minireceptor ectodomain has eight putative *N*-glycosylation consensus sites, we studied whether the minireceptor without the cytoplasmic domain is effectively *N*-glycosylated. Cells were incubated with or without tunicamycin, an inhibitor of *N*-glycosylation, pulse-labeled with [^{35}S]methionine/cysteine for 4 h, and the mLRP/LRPTmΔT immunoprecipitated with HA antibody. In control cells, three predominant bands are observed, corresponding to the Golgi precursor form and to the 120-kDa and 74-kDa mature forms generated after processing by furin (Figure 5C). In contrast, the tunicamycin-treated cells expressed only the low molecular weight precursor form (ER form) of the mLRP/LRPTmΔT. This result indicates that the minireceptor is effectively *N*-glycosylated. However, we could not assess the role of *N*-glycan in its apical sorting because under tunicamycin treatment the protein was arrested in the ER (Figure 5C). *N*-glycans seem to be

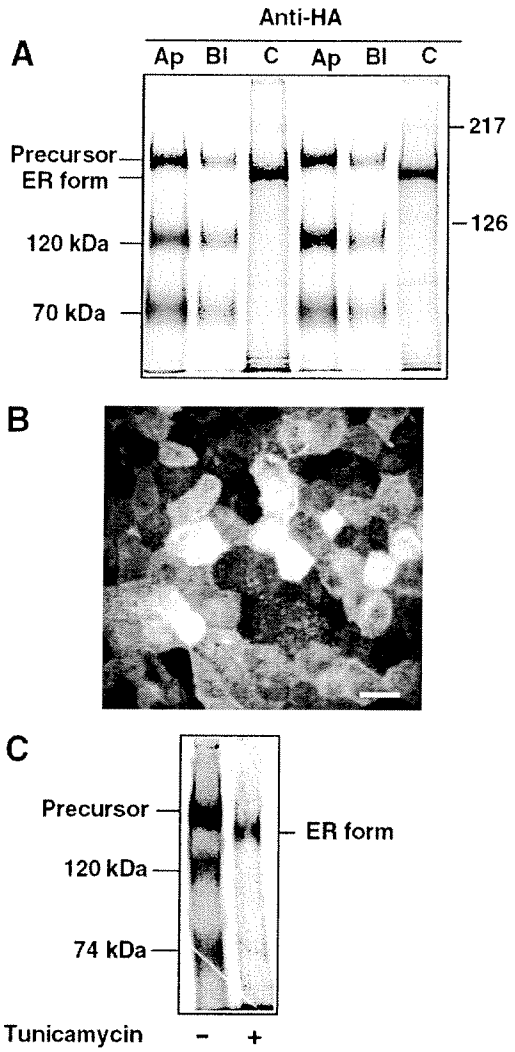

Figure 5: The minireceptor ectodomain contains apical sorting information. (A) Filter-grown MDCK cells expressing SmLRP were pulse-labeled with [^{35}S]methionine/cysteine for 60 min, chased for 4 h and lysed. The total cell lysate and the apical (Ap) and basolateral (Bl) media were immunoprecipitated with anti-HA antibody. The immunoprecipitates were resolved by 6% SDS-PAGE under reducing conditions. Two different clones are shown. (B) MDCK cells expressing mLRP/LRPTmΔT were grown on Transwell-clear filters and processed for indirect immunofluorescence microscopy without permeabilization. Primary anti-HA antibody and the secondary anti-mouse FITC were added to both sides of the filter. The label is predominantly apical as is shown in the picture representing the sum of ten 1.0-μm confocal microscopy xy sections (scale bar, 20 μm). (C) MDCK cells stably transfected with mLRP/LRPTmΔT were pulse-labeled with [^{35}S]methionine/cysteine for 240 min in the absence (–) or presence (+) of tunicamycin (10 μg/ml). Cells were lysed and immunoprecipitated with anti-HA antibody. The complexes were resolved in 6% SDS-PAGE under reducing conditions and bands were visualized by autoradiography.

required for the folding process of the receptor (McCormick and Bu, unpublished results). The different distribution achieved by the tailless minireceptor and the complete minireceptor indicates that the cytoplasmic domain of LRP harbors dominant basolateral sorting information.

To investigate the intracellular trafficking of mLRP/LRPTmT in MDCK cells, we traced the cell surface delivery of newly synthesized minireceptor using a pulse-chase/membrane targeting assay. Confluent MDCK monolayers were pulse-labeled with [^{35}S]methionine/cysteine for 30 min, chased for different time periods, biotinylated from either the apical or basolateral surface, lysed, and immunoprecipitated by HA antibody. The precipitated mLRP/LRPTmT molecules were subsequently precipitated by streptavidin-agarose, so that only the radiolabeled minireceptor that had reached the cell surface at the time of biotinylation was detected by autoradiography. After 60 min of chase, almost no minireceptor (less than 2% of the total) was detected on either surface (Figure 6A). At this time-point, we found that the majority of the newly synthesized protein was in the precursor form, with almost no mature forms (120-kDa and 85-kDa subunits) (Figure 6B). After 90 min of chase, mLRP/LRPTmT began to appear on the basolateral surface, as indicated by the 120-kDa band on SDS-PAGE analysis. It is evident that newly synthesized minireceptor containing the cytoplasmic domain of LRP was delivered predominantly to the basolateral plasma membrane at all time-points tested (Figure 6C), suggesting that the protein follows a direct route from the TGN to the basolateral domain. These results are consistent with the steady-state surface basolateral distribution of both endogenous LRP and the minireceptor mLRP/LRPTmT in MDCK cells.

The megalin cytoplasmic domain contains information for apical localization

Using a similar experimental approach for analyzing LRP sorting, we studied the role of the megalin cytoplasmic domain in the apical sorting of the protein. The minireceptor mLRP/LRPTmMegT was expressed in MDCK cells. As is shown in Figure 7, the chimeric minireceptor was distributed apically in MDCK cells. Most of the protein at the cell surface, which was the target of the biotinylation procedure, was the mature 120-kDa subunit, while in the cell lysate, both the precursor and the mature forms were found (Figure 7A). The distribution of the mLRP/LRPTmMegT in polarized MDCK cells is also illustrated in Figure 7(B). By indirect immunofluorescence, the protein was detected in a punctate pattern in the apical portion of the cell. This result indicates that, at steady-state, mLRP/LRPTmMegT is localized in the apical domain of the cell.

Although the chimeric protein has a clear apical distribution, the fact that the minireceptor ectodomain conveys an apical determinant (Figure 5A,B) made it necessary to determine if

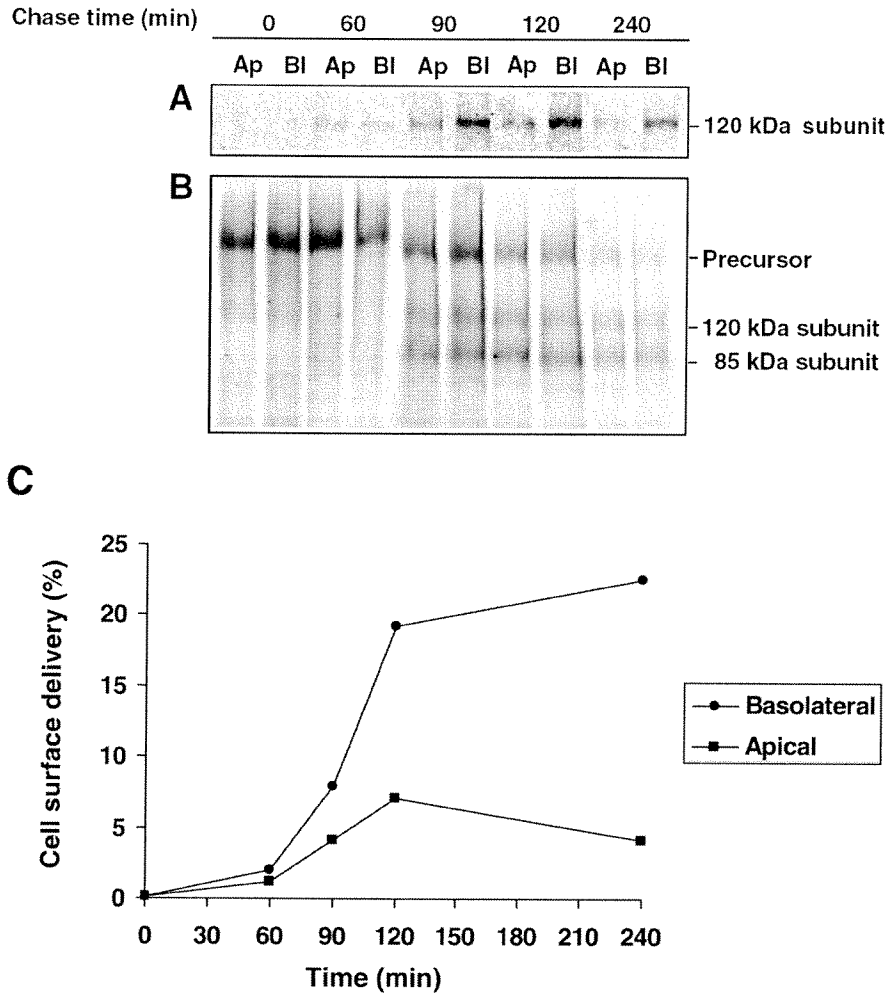

Figure 6: Processing and targeting of mLRP/LRPTmT directly to the basolateral membrane. Vectorial delivery of mLRP/LRPTmT to the cell surface was analyzed by a membrane targeting assay (see Experimental Procedures). Cells grown on filters were pulse-labeled with [^{35}S]methionine/cysteine for 30 min. At various time-points during the chase, metabolically labeled minireceptor expressing MDCK cells were biotinylated from either the apical (Ap) or basolateral (Bl) surface and immunoprecipitated with anti-HA monoclonal antibody. (A) Biotinylated, radiolabeled immunoprecipitates were obtained by subsequent reprecipitation of 4/5 parts of the total immunoprecipitated sample with streptavidin-agarose. (B) For each chase time, a fraction (1/5) of the immunoprecipitate sample was analyzed by 6% reducing SDS-PAGE and shown as total immunoprecipitate. (C) Fluorograms of (A) and (B) were scanned and quantified using NIH image program for Windows, and the results obtained were corrected by the fraction of the total immunoprecipitated sample that was loaded on the gels [4/5 for (A) and 1/5 for (B)]. The resulting numbers were used to calculate the percentages of the total labeled protein that are in the cell surface (biotinylated) for each time-point. It should be noted that the gel was slightly overexposed for the purpose of clearly visualizing the bands but not for the quantification analysis.

the tail is sufficient to mediate apical targeting of an unrelated protein with no known apical determinants. To address this issue, we expressed a chimeric protein containing the megalin tail with HA-tagged GFP as the ectodomain in MDCK cells. The expression of the construct in the stably transfected cells was confirmed by Western blot and flow cytometry analysis. We seeded the resulting transfectants onto coverslips and Costar Transwell filters, and determined if GFP/MegTmT was targeted to the apical portion of the cell. As shown in Figure 8(A), by indirect immunofluorescence using anti-HA, the GFP/MegTmT labeling, in non-permeabilized cells, was in a fine vesicular pattern characteristic for apical staining. With permeabilized cells, we did not detect label corresponding to the basolateral membrane. We also analyzed the GFP/MegTmT localization in confluent monolayers by confocal microscopy. Panel B of Figure 8 shows the distribution pattern of GFP/MegTmT from three sections, starting from the apical domain to the basal domain. The majority of the label is in the apical pole with some appearing intracellularly. By cell surface biotinylation, it was confirmed that the chimeric protein appeared exclusively in the apical domain. E-cadherin, an endogenous marker of the basolateral domain, was localized correctly in the same filter grown cells (Figure 8C). The construct

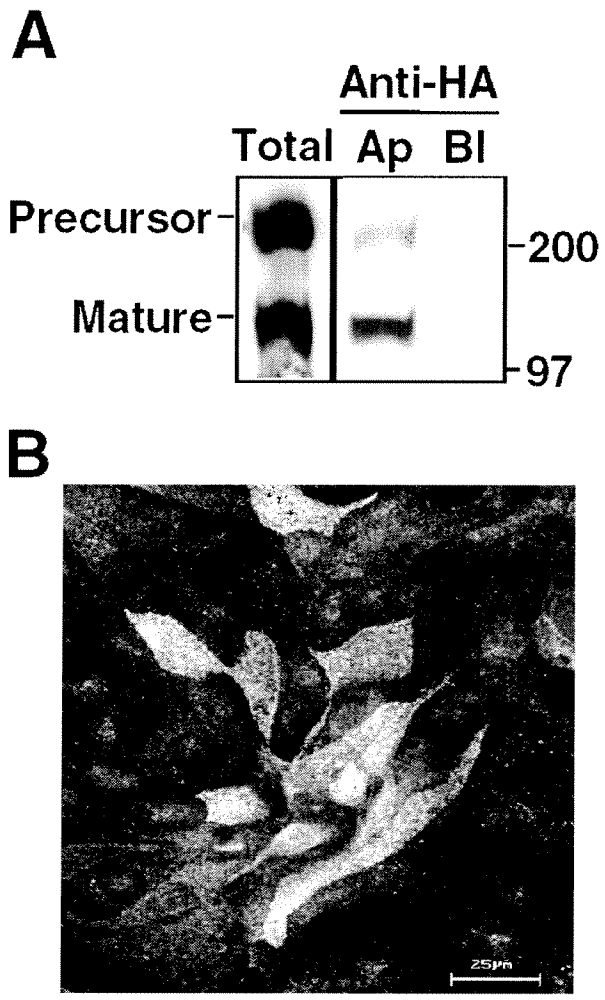

Figure 7: Apical expression of a minireceptor containing the megalin cytoplasmic domain. Permanent transfectants of MDCK cells forming impermeable monolayers in Transwell chambers were analyzed for the polarized expression of mLRP/LRPTmMegT as described in Figure 4. (A) Cells were selectively biotinylated and the cell lysates were treated as described in Experimental Procedures. The minireceptor was detected by Western blot using an anti-HA antibody. The majority of the protein on the surface is the mature form, compared with the total lysate where the precursor form is also found. (B) mLRP/LRPTmMegT-expressing MDCK cells grown on coverslips were fixed, permeabilized and incubated with anti-HA overnight at 4 °C. After incubation with the secondary antibody (anti-mouse IgG conjugated with FITC), cells were mounted and analyzed for immunofluorescence staining. The minireceptor is mainly restricted to the apical surface.

GFP/LRPTmMegT was also localized apically in transfected MDCK cells (Figure 8A,B). Since this chimeric protein contains the transmembrane domain of LRP instead of megalin, this result strongly suggests that its apical localization is due to the presence of the megalin cytoplasmic domain.

To exclude the possibility that the ectodomain of the GFP/MegT constructs harbor apical sorting information, such as *N*-glycosylation, we used two different experimental approaches. First, we incubated MDCK cells expressing GFP/MegTmT with tunicamycin overnight and during a 240-min [^{35}S]methionine pulse labeling, followed by HA immunoprecipitation of the cell lysate. This treatment did not change the molecular size of the radiolabeled protein (Figure 9A), indicating that the ectodomain of GFP is not glycosylated. As a second approach, we generated a MDCK cell-line expressing the soluble protein, HA-tagged GFP (GFPsec). We performed a pulse-chase experiment with the cells seeded on filters and the polarity of GFPsec secretion was assessed by immunoprecipitation of the apical and basolateral media with HA antibody. As shown in Figure 9(B), GFPsec is secreted with no polarity, demonstrating that the ectodomain does not contain apical sorting information. This result is also important to exclude the possibility that the default localization of MDCK is to the apical domain.

The association of membrane proteins with detergent-insoluble glycosphingolipid complexes (DIGs or lipid rafts) sometimes correlates with their apical localization. In order to determine if megalin and the megalin chimeric proteins interact with DIGs, we examined their distribution via sucrose density gradients, and compared it to that of caveolin 1, which partitions into lipid rafts (40). We found that a small portion (18%) of endogenous megalin from LLC-PK1 cells floated in fractions 5–8 (20–34% sucrose) corresponding to lipid rafts (Figure 10A,E). Twenty-four per cent of the chimeric protein GFP/MegTmT, expressed in MDCK cells, was found in the lipid rafts fractions (Figure 10E). However, as with endogenous megalin, an important fraction of the chimeric protein partitioned in the bottom of sucrose gradients (Figure 10E), where the nonraft protein E-cadherin was found (Figure 10B). The raft association was probably due to the presence of the megalin transmembrane domain and was not required to achieve apical localization. In fact, both the minireceptor mLRP/LRPTmMegT and the chimeric protein GFP/LRPTmMegT, which contain the transmembrane domain of LRP, fractionated completely to the bottom of the sucrose density gradients (Figure 10C,D). These experiments reveal that the apical localization of megalin and the chimeric megalin tail proteins is not dependent on their association with lipid rafts and/or the presence of the megalin transmembrane domain.

Discussion

In this report we studied the distribution of two giant receptors of the LDL-R family, LRP and megalin, in polarized renal epithelial cell lines, MDCK and LLC-PK1. We also investigated the molecular determinants in the receptors that dictate their polarized localization. Both receptors contain four clusters of cysteine-rich complement-type/LDL-R class A repeats in their ectodomains, and are similar

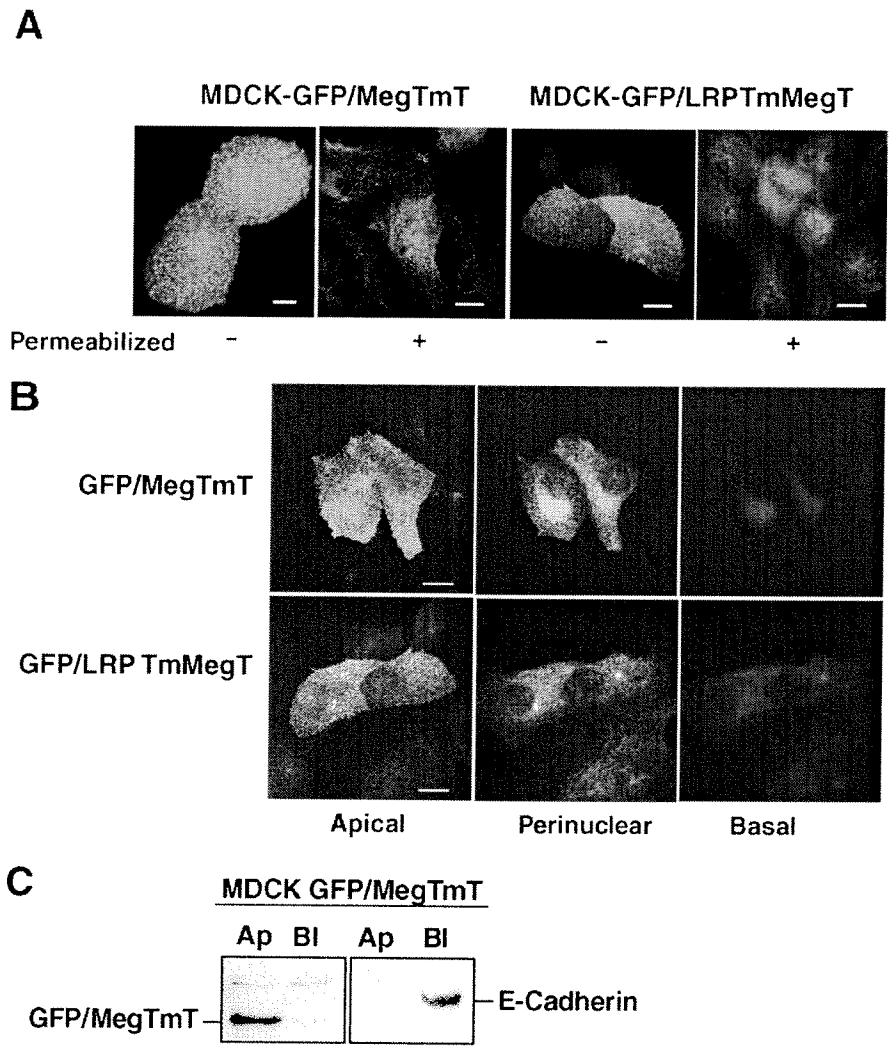

Figure 8: Apical expression of GFP-MegT transfected MDCK cells. MDCK cells expressing the constructs GFP/MegTmT and GFP/LRPTmMegT were grown on coverslips (A,B) or filters (C) to analyze the distribution of the chimeric protein. (A) Cells expressing the chimeric protein were fixed and labeled with an anti-HA antibody to label the ectodomain of the chimeric proteins. (B) Confocal images acquired from confluent cells expressing GFP chimeric proteins; three sections corresponding to the apical, perinuclear and basal planes of the polarized monolayer are shown. (C) Cell surface biotinylation of MDCK cells expressing GFP/MegTmT and detected by Western blot, show the apical distribution of the 52-kDa chimeric protein. As a control for cell polarization, the PVDF membrane was stripped and blotted with rat anti-E-Cadherin to localize this endogenous basolateral protein (scale bar, 5 μm).

in terms of the binding to and internalization capacity for certain ligands in solid-phase assays and cell culture (41–43). However, their overall physiological functions are very different (44), as is reflected in the knock-out models (8, 9, 15, 45) and in human and animal models for receptor dysfunction (45–47). We hypothesized that this functional disparity of the receptors could be partially explained by their opposite distribution in polarized cells within several tissues where they are both expressed.

If both receptors are compared structurally, their major differences are present in their cytosolic domains, which are relatively small compared to the ectodomains. LRP has a cytoplasmic domain composed of 100 amino acids, with one phosphorylation site for PKA (6), three tyrosine-based motifs, and two dileucine motifs (5). The megalin cytoplasmic domain has 209 amino acids and harbors several interesting motifs, including three putative endocytosis motifs (one dileucine, two NPxY and one Yxxϕ motifs), phosphorylation sites for PKC and PKA, SH3 proline rich motifs and one SEV sequence in the carboxyl-terminal part of the tail, which constitutes a PDZ motif. For this reason we searched for sorting information in the tail of both receptors.

First, we demonstrated that LRP is basolaterally located in MDCK cells. By using different minireceptors, we showed that the basolateral information resides in the cytoplasmic domain of the receptor. In fact, the minireceptor containing the entire LRP cytoplasmic domain (mLRP/LRPTmT) showed a predominant basolateral distribution, whereas the minireceptor mLRP/LRPTmΔT lacking the cytosolic tail had a predominant apical distribution, probably due to residual sorting information in the *N*-glycosylated ectodomain. The basolateral signal present in the tail is dominant over the apical signal of the tailless minireceptor. Moreover, this addressing information directly targeted the minireceptor to the basolateral domain, suggesting that it is recognized by the sorting machinery within the biosynthetic pathway, mostly at the TGN.

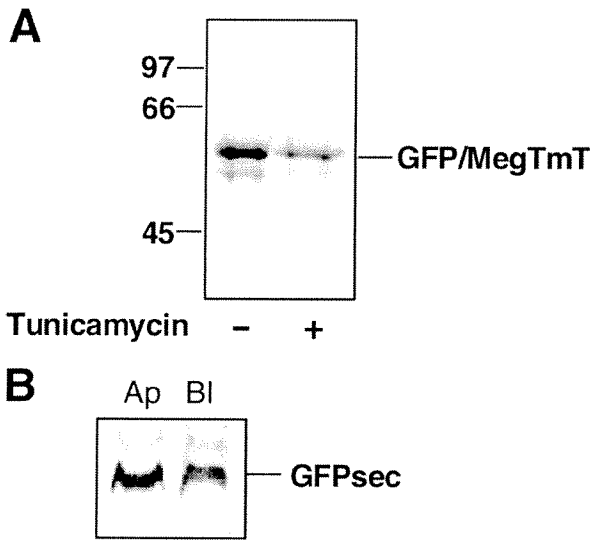

Figure 9: The ectodomain of the chimeric proteins GFP/MegTmT does not contain apical sorting information. (A) MDCK cells expressing GFP/MegTmT were pulse-labeled with [^{35}S]methionine/cysteine for 240 min in the absence (–) or presence (+) of tunicamycin (10 μg/ml). Cells were lysed and immunoprecipitated with anti-HA antibody. The complexes were resolved in 10% SDS-PAGE and the 52-kDa band was visualized by autoradiography. (B) Filter-grown MDCK cells expressing GFPsec were pulse-labeled with [^{35}S]methionine/cysteine for 60 min, chased for 4 h and lysed. The apical (Ap) and basolateral (Bl) media were immunoprecipitated with anti-HA antibody. The immunoprecipitates were resolved by 15% SDS-PAGE.

The expression of LRP in the somatodendritic domain in neurons and its basolateral distribution in MDCK cells is coincident with the hypothesis establishing that the mechanisms controlling sorting in epithelial and neuronal cells may be similar (48). Another family member, LDL-R, is also expressed in the basolateral domain in several epithelial cells, including MDCK (49) and is somatodendritic in neurons (34). This receptor has two independent basolateral sorting signals, a weak, tyrosine-based one that overlaps with the endocytosis motif (NPxY) and a dominant one, also tyrosine-based, not related to the endocytosis signal (37), (see Figure 3A).

LRP showed a nonpolarized distribution in the μ1B defective cell line LLC-PK1, but this localization was reverted to the basolateral domain in LLC-PK1 transfected with the missing adaptor subunit of the AP-1B complex. There is some evidence suggesting that μ1B participates in the sorting of basolateral proteins with tyrosine-based signals, such as LDL-R (35, 36), although it is not clear if it functions in the biosynthetic and/or recycling sorting pathway (50, 51). Therefore we studied the participation of the two tyrosines present in the LRP tail in the basolateral sorting of the receptor. Our results suggest that both tyrosine residues could be part of basolateral determinants (Y29 in the NPTY motif and Y63 in either NPVY and/or YATL motifs). In addition, resembling the characteristic of the distal strongest basolateral sorting signal of the LDL-R (37), the Y29 is also close to a pair of acidic residues that therefore might contribute to conform the basolateral sorting signal of LRP.

Our results suggest that both Y29 and Y63 could play a role in different stages of the LRP basolateral pathway. The basolateral steady-state distribution of an endocytic protein, such as LRP, is a result of at least two signal-mediated trafficking pathways. In the biosynthetic route, the receptor has to be segregated into basolateral directed vesicles, probably at the TGN. Once in the plasma membrane, the receptor is constitutively internalized and has to be sorted at the basolateral recycling endosome back to the basolateral plasma membrane. The first NPxY motif could participate as a TGN to basolateral plasma membrane sorting signal, explaining why we did not find any basolateral localization of the Y29A mutated minireceptor. Y63 is part of the dominant endocytic motif of LRP, YATL (5). This tyrosine, as part of either NPVY and/or YATL motifs, could have a role in the basolateral recycling of the minireceptor, maintaining the correct localization of the protein after endocytosis, where μ1B could participate (51). We are currently investigating in detail the nature of the basolateral signal in the LRP cytoplasmic domain and the role of the different motifs in trafficking pathways within polarized epithelial cells.

In the case of megalin, it is already known that this receptor is apically distributed in several epithelial tissues. However, the molecular determinant of its apical localization has not been examined. Our results clearly show that the tail of megalin harbors information for its apical localization in spite of the presence of several putative basolateral motifs such as LL, two NPXY motifs and one Yxxϕ motif in the cytosolic domain of the receptor (Figure 3A). Since, the ectodomain of basolateral receptors normally expresses recessive apical sorting information (27), as we also show for the minireceptor, we used GFP as a reporter ectodomain. GFP itself does not have an apical sorting determinant, as a secreted form of GFP was equally secreted by the two plasma membrane domains. The two chimeric proteins containing the cytoplasmic domain of megalin and GFP in the ectodomain with either the transmembrane domain of megalin or the transmembrane domain of LRP were localized in the apical domain of MDCK cells. These chimeric proteins are not *N*-glycosylated, as was shown in the tunicamycin experiment, eliminating the possibility of the presence of this apical sorting information in the ectodomain. The fact that the chimeric protein GFP/LRPTmMegT is apically localized strongly suggests that the megalin cytoplasmic domain contains apical sorting information. We do not know yet if the information for apical localization determines the direct or indirect targeting of the protein to the apical membrane and/or its apical retention. This is an important aspect in the field of cell polarity, since both the protein signals and the cell machinery for apical sorting have been elusive. The known examples of apical

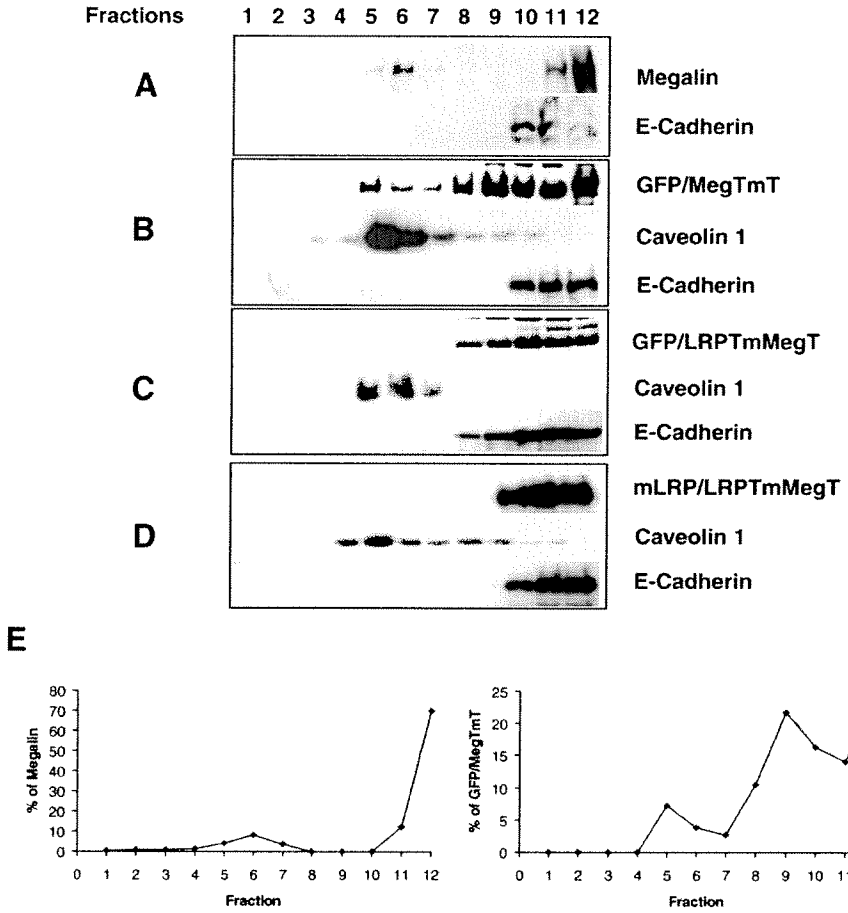

Figure 10: Megalin and the chimeric protein containing megalin transmembrane domains are present in lipid rafts. LLC-PK1 cells expressing endogenous megalin and MDCK cells expressing either GFP/MegTmT, GFP/LRPTmMegT or mLRP/LRPTmMegT were extracted with 1% Triton X-100, and the resulting cell lysates were centrifuged to equilibrium in a sucrose gradient, as described in Experimental Procedures. Aliquots from each fraction were subjected to SDS-PAGE and analyzed by immunoblotting. Both megalin in LLC-PK1 cells (A) and GFP/MegTmT in MDCK cells are present in lipid rafts fractions (5–8), the same fractions where caveolin is found (middle in B). In contrast, neither GFP/LRPTmMegT (C) nor mLRP/LRPTmMegT (D) was associated with lipid rafts in MDCK cells. As controls for raft and non-raft fractions, the distribution of caveolin 1 and E-cadherin was determined in all sucrose gradients from MDCK cells. (E) The amount of megalin and GFP/MegTmT present in each fraction of the gradients is reported as a percentage of the total amount of the protein in all fractions. The data are representative of several independent experiments (two for measuring megalin in LLC-PK1 and four for GFP/LRPTmMegT in MDCK cells).

proteins with a cytosolic tail localization determinant are almost all polytopic, with the exception of endotubin (52) that could have a cytosolic apical sorting determinant that drives the protein to the apical early endosome. For rhodopsin, it was shown that the apical signal allows the direct targeting of the protein to the apical membrane (29). CFTR (53) and cMOAT (54) are other examples of polytopic apical proteins with a localization signal in their cytosolic domain. For CFTR it has been shown that a PDZ motif in the carboxy terminus is required to maintain its apical localization. Through this motif, the protein interacts with EBP50/NHERF (53) and with the E3KARP-ezrin complex that could be important in stabilizing CFTR at the apical membrane domain (55). As was mentioned, megalin has a PDZ motif (SEV) that binds to some PDZ proteins (56, 57) that could have a role as an anchoring element. The megalin cytoplasmic domain also harbors a proline-rich SH3 binding motif, homologous to one present in the amiloride-sensitive sodium channel that determines its apical localization through an interaction with the actin cytoskeleton (30). We are currently investigating the role of different megalin tail motifs in the apical localization of the receptor.

Finally, we have to consider that the *N*-glycosylated ectodomain of megalin could participate in its apical localization (58). Also, we cannot dismiss a possible role for the transmembrane domain, as a small fraction of both endogenous megalin and the GFP/MegTmT chimeric protein partition into lipid rafts floated in sucrose gradients in the presence of triton X-100. The association with lipid rafts is linked to the apical localization of several proteins in epithelial polarized cells (59, 60). However, megalin tail chimeric

proteins that did not associate with rafts also localized at the apical domain (see Figure 10C,D) indicate that stable binding to lipid rafts is not a requirement for apical sorting as has been suggested for other apical proteins (61, 62). In this regard, megalin could have more than one way of ensuring its apical localization, which is necessary to accomplish its important physiological functions.

Materials and Methods

Materials

All tissue culture media, serum, and plasticware were from Life Technologies, Inc (Rockville, MI, USA). Tissue culture-treated Transwell polycarbonate filters were from Costar (Costar, Cambridge, MA, USA). Rabbit polyclonal anti-human LRP and the monoclonal anti-HA antibody have been described before (63). Polyclonal anti-human megalin was generated against a recombinant megalin tail obtained as described below. Monoclonal anti-gp135 antibody was a generous gift from Dr George Ojakian (SUNY Downstate Medical Center, NY, USA). Rat anti-uvomorulin/E-cadherin monoclonal antibody was from Sigma (Sigma Chemical, St. Louis MO, USA). Rabbit polyclonal anti-human caveolin IgG was from Santa Cruz Biotechnology (Santa Cruz, California, USA). The goat anti-mouse IgFITC was from Dako (Dako Cytomation, Denmark A/S, Denmark). Goat anti-rat IgCy3 was from Chemicon International (Temecula, CA, USA). Cy3-conjugated goat anti-mouse IgG and Cy3 conjugated goat anti-rabbit IgG was from Amersham Pharmacia Biotech (Piscataway, NJ, USA). Sulfo-NHS-LC-biotin and Immunopure Streptavidin-agarose was from Pierce (Rockford, IL, USA). ProteinA-agarose was from Repligen (Waltham, MA, USA). Peroxidase-labeled anti-mouse antibody and the ECL system were from Amersham Pharmacia Biotech. Immobilon-P transfer membrane was from Millipore (Billerica, MA, USA). Rainbow molecular weight markers were from Bio-Rad (Hercules, CA, USA). Restriction enzymes were from Promega (Madison, WI, USA) and Pfu DNA polymerase from Fermentas (Vilnius, Lithuania).

Expression and purification of recombinant GST/LRP-tail for antibody production

For GST/MegT fusion protein, the cDNA that encodes the entire megalin tail was generated via PCR from a human kidney cDNA library (BD Biosciences Clontech, Palo Alto, CA, USA) and subcloned into the GST expression vector pGEX-2T (Amersham Life Science). GST/Meg-tail fusion protein was expressed in *Escherichia coli* (BL21) and purified essentially according to the manufacturer's instructions (Amersham-Pharmacia Biotech) except with the addition of Complete™ (Boehringer Mannheim, Mannheim, Germany) protease inhibitor cocktail in the lysis buffer (PBS, 1% Triton X-100, 10 mM EDTA). All the purified proteins were dialyzed against 50 mM Tris-HCl pH 8.0. The megalin cytoplasmic domain was released from the GST fusion protein by incubation with thrombin (Sigma). The resulting megalin fragment was used to produce antibodies in rabbit.

Construction of chimeric minireceptors

All the constructs have the HA epitope in their amino termini. The construction of mLRP/LRPTmT, mLRP/LRPTmMegT mLRP/LRPTmΔT and the mutants mLRP/LRPTmT Y29A and Y63A have already been described (5, 63, 64). The construct encoding the soluble form of the minireceptor, SmLRP, was made with mLRP/LRPTmT as a template and amplifying by PCR part of its ectodomain between the EcoR I site and the base just before the sequence of the transmembrane domain. The 3′ primer includes a stop codon and a Xho I site. mLRP/LRPTmT and the PCR product encoding the secreted ectodomain were digested with EcoR I and Xho I. The PCR product was ligated with the purified plasmid devoid of its insert. The PCR primers were SmLRP 5′: 5′-GATCGAATTCAGCTGCGCCACCAATGCCAGCA-3′, SmLRP 3′: 5′-GATCCTCGAGCTATCCTGGCTGCTGCTGG-CTGAAG-3′. The construction of GFPsec was performed by replacing the ectodomain of SmLRP (between BamH I and Xho I) with a DNA corresponding to GFP but without the initiation codons. The DNA was amplified by PCR using the plasmid pEGFP (ClonTech) as template. The 5′ primer includes a BamH I site and eliminates the ATG from GFP and was the same for all the GFP constructs. The 3′ primer contains the stop codon and a Xho I site. The sequences of the primers were: GFPsec 5′: 5′GATCGGATCCGTGAGCAAGGGCGAGGAGCT 3′. GFPsec 3′: 5′GATCCTCGAGTTACTTGTACAGCTCGTCCATGCC 3′. The construct GFP/MegTmT was made using a method similar to that used to make GFPsec but the receptor plasmid was mLRP/LRPTmT cut with BamH I and Xho I to eliminate the sequence corresponding to the minireceptor ectodomain. The GFP insert was created by PCR using pEGFP (ClonTech) as a template. The 3′ primer contains the Xho I site but without a stop codon. The minireceptor expression construct mLRP/LRPTmT was developed using a strategy similar to that described previously for mLRP/LRPTmMegT (64), except the corresponding DNA fragment of megalin transmembrane and cytosolic domains was obtained by PCR, using a human kidney cDNA library (ClonTech). The primers used for the PCR amplification of the cDNA fragment are megalin Tm-T 5′: 5′-GATCCTCGAGGTAGCTGTGCTGTTGACAATCCTC-3′ and megalin Tm-T 3′: 5′-GATCTCTAGACTATACTTCAGAGT-CTTCTTTAACA-3′. Finally, the GFP/LRPTmMegT was done by inserting the PCR product GFP-LRP Tm nonstop into the plasmid mLRP/LRPTmMegT cut with BamH I and XhoI, to eliminate the sequence encoding the ectodomain and transmembrane domains of the minireceptor. The resulting construct is similar to the GFP/MegTmT, but with the transmembrane domain of LRP instead of megalin. The 3′ primer included the complete transmembrane domain of LRP and the Xho I site. The sequence of the 3′ primer of GFP-LRP Tm nonstop

was: 5'GATCCTCGAGATACCAGAATACCACTCCGGCCAC-CAGAACCAGCAGCAGCAGCAACAGCAGAGGGATTAGGA-TGGAGGCTATATGCTTGTACAGCTCGTCCATGCC 3'. All the constructs were verified by DNA sequencing.

Cell culture and transfection

MDCK cells (strain II) were maintained in DMEM (Life Technologies) supplemented with 7.5% fetal bovine serum (FBS) (Life Technologies) containing 100 U/ml penicillin and 100 mg/ml streptomycin sulfate. LLC-PK1 cells were grown in αMEM (Life Technologies), 10% FBS, 2 mM glutamine and penicillin-streptomycin. LLC-PK1 μ1B (provided by Dr Enrique Rodriguez-Boulan) (51) were grown in the same media as the wild-type cells plus 0.2 mg/ml of G418. Clonal cell lines were derived from MDCK cells stably transfected with 2 μg DNA by using Lipofectamine Plus transfection reagent (Life Technologies) according to the supplier's protocol, followed by 10–14 days of selection with 0.8 mg/ml of G418 (Life Technologies). Cells were screened and analyzed by Western blot, flow cytometry, indirect immunofluorescence or direct fluorescence of GFP, as described below. Selected clones were maintained in the same medium plus 0.4 mg/ml of G418.

For most experiments related to polarity analysis, cells were plated at high density onto 12- or 24-mm Transwell polycarbonate filters units (0.4-μm pore size). Cells were grown until the transepithelial resistance reached 200–350 ohm/cm^2 for MDCK cells, 150–250 ohm/cm^2 for the LLC-PK1 cells, and 2500–3000 ohm/cm^2 for LLC-PK1 expressing μ1B, as measured with an EVOM electrometer (World Precision Instruments, Sarasota, FL, USA). The formation of a properly polarized monolayer of MDCK cells was determined by the analysis of the lateral expression of E-cadherin or the apical expression of gp135, either by indirect immunofluorescence or by biotinylation, as was required.

Pulse-chase and Western blot analyses of LRP, megalin and minireceptors

Pulse-chase analysis of mLRP/LRPTmT, mLRP/LRPTmΔT, mLRP/LRPTmMegT, SmLRP or GFP-MegTs stably expressed in MDCK cells was performed essentially as described (63). When tunicamycin was used, cells were incubated in the presence of the drug 12 h before the experiment (2 μg/ml) and then during depletion and pulse labeling (10 μg/ml). To assess the polarity of the secretion of the SmLRP and of GFPsec, transfected MDCK cells were grown on filters until they reached confluency, as was described. Cells were incubated twice with depletion medium (DMEM without methionine and cysteine) and then pulsed with 150–200 μCi of [^{35}S]methionine/cysteine (NEN) in 120 μl of medium applied to the basolateral side of the inverted filter (28). After 4 h of chase in complete medium containing 10-fold increased concentrations of methionine (3 mg/ml) and cysteine (6.5 mg/ml), immunoprecipitations with anti-HA monoclonal antibody were made for the apical and basolateral media, as described (65). Immunoprecipitates were resolved in SDS-PAGE (6% for SmLRP, 15% for GFPsec) and the bands visualized by autoradiography.

For Western blotting, cells were lysed with lysis buffer (phosphate-buffered saline containing 1% Triton X-100, containing 1 mM PMSF, 1 μg/ml each of pepstatin, antipain, leupeptin) for 30 min at 4 °C. Equal quantities of protein were subjected to SDS-PAGE under reducing conditions. Following transfer to polyvinylidene difluoride (PVDF) membrane, successive incubations with the corresponding primary antibody (anti-HA 1 : 500, anti-megalin tail 1 : 2000, anti-human LRP 1 : 500, anti-gp135 1 : 100, anti-caveolin 1 1 : 3000 and anti-E-cadherin 1 : 1000), horseradish peroxidase-conjugated anti-mouse, anti-rabbit or anti-rat IgG (1 : 10000) were carried out for 60 min at room temperature. The immunoreactive proteins were detected using the ECL system.

Cell surface expression of LRP, megalin and minireceptors in polarized cell lines

The cell surface distribution of the receptors was assessed by performing both biochemical and microscopy experiments. Cell surface biotinylation was performed at 4 °C essentially as described (66). Briefly, the cell monolayers grown on filters were washed in PBSc (PBS containing 1 mM calcium and 1 mM magnesium) and then biotinylated with sulfo-NHS-LC-biotin from either the apical (0.7 ml) or basolateral (1.5 ml) chamber compartment. The chamber not receiving biotin was incubated with PBSc. Filters were incubated twice for 30 min. After biotinylation steps, biotin was quenched by incubation with 50 mM NH_4Cl in PBSc for 10 min. Cells were lysed in ice-cold lysis buffer (150 mM NaCl, 20 mM Tris, pH 8.0, 5 mM EDTA, 1% Triton X-100, 0.2% BSA, and protease inhibitors). Biotinylated cell surface proteins were then adsorbed to streptavidin-agarose beads for 2 h. Beads were washed and then the biotinylated proteins were analyzed by SDS-PAGE followed by immunoblotting as was described above.

For microscopy, the cells were grown either on filters or on glass coverslips. The confluent monolayer was fixed in 4% paraformaldehyde in PBSc and then permeabilized or not with 0.2% Triton X-100 in PBSc. Before being incubated with the primary antibody, cells were blocked with 0.2% gelatin in PBSc. Successive incubations with the first antibody and Cy3 or FITC-conjugated secondary antibody were carried out. After washing with 0.2% gelatin in PBSc and PBSc, the coverslips or filters were mounted with Mowoil (Calbiochem, San Diego, CA, USA) and the preparations were examined using a fluorescent microscope or a laser confocal microscope. For non-permeabilized cells grown on filters, the primary and secondary antibodies were incubated sequentially in PBS-gelatin on both sides of the filters. For GFP-MegT-expressing cells, either direct fluorescence of fixed cells or anti-HA immunofluorescence was performed. Immunofluorescence was observed and analyzed with a Zeiss laser scanning

confocal microscope (Zeiss Axiovert 200 M microscope and LSM 5 Pascal laser scanning confocal). Typically 24 serial images were taken in 0.6-μm steps or 12 serial images in 1-μm steps, beginning 1–2 μm below the focal plane of the bottom of the monolayer and proceeding upward to 1–2 μm above the top of the monolayer.

Targeting of the mLRP/LRPTmT to the cell surface in polarized MDCK cells

The procedure followed was developed by Le Bivic as described (66). Cells were grown on filters until confluency. They were pulse-labeled for 30 min in depletion medium containing [^{35}S]methionine/cysteine at 37 °C and chased with complete medium at different times (0, 60, 90 and 120 min), essentially as described (28). After the chase time, cells were kept in ice-cold $NaHCO_3$-DMEM containing 20 mM HEPES and 0.2% BSA and then biotinylated as described. The cells were lysed in PBS 1% Triton X-100 with protease inhibitors, and the lysate was subject to immunoprecipitation using anti-HA antibody. The complexes were then precipitated with proteinA-sepharose for 2 h at 4 °C. After washing, the immune complexes were dissociated by adding 10% SDS and boiling for 5 min and diluted with 1 ml of lysis buffer. One fifth of the sample was taken to measure the total label incorporation to the protein, and the remaining sample was centrifuged to take the supernatant. The biotinylated minireceptor was precipitated by the addition of streptavidin-Sepharose. After washing the beads, the labeled proteins were resolved on 6% SDS-PAGE under reducing conditions, dried and exposed for autoradiography. Densitometry analysis was carried out within the linear range of the film using the NIH image program for Windows.

Analysis of rafts association by sucrose gradients

Detergent-resistant membranes were isolated using a modification of the standard procedure (25). Briefly, cells grown to confluence in 100-mm plates were rinsed three times with PBSc and carefully scraped in PBSc. Cells were centrifuged in a microfuge at 2000 r.p.m. for 10 min and lysed for 60 min in 0.5 ml of lysis buffer TNE-T (25 mM Tris-HCl, 5 mM EDTA, 150 mM NaCl, pH 7.5, 1% Triton X-100) with protease inhibitors at 4 °C. The lysate was homogenized by passing the sample through a 22-gauge needle. The extract was finally brought to 40% sucrose in a final volume of 1 ml and placed at the bottom of a 5-ml 5–35% sucrose gradient. Gradients were centrifuged in a Sorvall AH650 rotor at 46000 r.p.m. for 18 h. Fractions (0.4 ml each) were harvested from the top, and proteins were recovered by TCA precipitation. The TCA pellets were washed twice with ethanol-ether 1 : 1, dried and diluted in sample buffer. Samples were subjected to SDS-PAGE under reducing conditions (15% for GFP-MegT and caveolin, 5% for megalin and 6% for E-cadherin). Gels were transferred to PVDF to detect the proteins by Western blotting and ECL. In order to quantify the percentage of the protein that floats to the raft-enriched fractions, densitometry analysis was carried out within the linear range of the scanned films using the NIH image program for Windows.

Acknowledgments

We thank Dr George Ojakian (SUNY Downstate Medical Center, NY, USA) for the generous gift of the gp135 antibody, Dr Carlos Vio (Biological Science Faculty, Pontificia Universidad Católica de Chile) for providing the LLC-PK1 cells and Dr Enrique Rodriguez-Boulan (Cornell University, NY, USA) for giving us the transfected cell line LLC-PK1 μ1b. We would also like to thank Elena Tetreault, Dr Alfonso Gonzalez, Dr Jorge Garrido for critical reading of the manuscript and Benjamin Erranz for his help in the manuscript editing. This work was supported in part by grants #1020746 from the Fondo Nacional de Investigación Científica y tecnológica (FONDECYT) to MPM, by FONDAP grant 13980001 to MPM, by a Conycyt grant to MIY and by the National Institutes of Health (NIH) to GB.

References

1. Howell BW, Herz J. The LDL receptor gene family: signaling functions during development. Curr Opin Neurobiol 2001;11:74–81.
2. Liu CX, Musco S, Lisitsina NM, Forgacs E, Minna JD, Lisitsyn NA. LRP-DIT, a putative endocytic receptor gene, is frequently inactivated in non-small cell lung cancer cell lines. Cancer Res 2000;60:1961–1967.
3. Herz J, Kowal RC, Goldstein JL, Brown MS. Proteolytic processing of the 600 kd low density lipoprotein receptor-related protein (LRP) occurs in a *trans*-Golgi compartment. EMBO J 1990;9:1769–1776.
4. Willnow TE, Moehring JM, Inocencio NM, Moehring TJ, Herz J. The low-density-lipoprotein receptor-related protein (LRP) is processed by furin *in vivo* and *in vitro*. Biochem J 1996;313:71–76.
5. Li Y, Marzolo MP, Kerkhof P, Strous GJ, Bu G. The YXXL motif, but not the two NPXY motifs, serves as the dominant endocytosis signal for LDL receptor-related protein (LRP). J Biol Chem 2000;275:17187–17194.
6. Li Y, van Kerkhof P, Marzolo MP, Strous GJ, Bu G. Identification of a major cyclic AMP-dependent protein kinase A phosphorylation site within the cytoplasmic tail of the low-density lipoprotein receptor-related protein: implication for receptor-mediated endocytosis. Mol Cell Biol 2001;21:1185–1195.
7. Hussain MM, Strickland DK, Bakillah A. The mammalian low-density lipoprotein receptor family. Annu Rev Nutr 1999;19:141–172.
8. Herz J, Couthier DE, Hammer RE. LDL receptor-related protein internalizes and degrades uPA-PAI-1 complexes and is essential for embryo implantation. Cell 1992;71:411–421.
9. Herz J, Couthier DE, Hammer RE. Correction: LDL receptor-related protein internalizes and degrades uPA-PAI-1 complexes and is essential for embryo implantation [letter]. Cell 1993;73:428.
10. Ulery PG, Beers J, Mikhailenko I, Tanzi RE, Rebeck GW, Hyman BT, Strickland DK. Modulation of beta-amyloid precursor protein processing by the low density lipoprotein receptor-related protein (LRP). Evidence that LRP contributes to the pathogenesis of Alzheimer's disease. J Biol Chem 2000;275:7410–7415.
11. Goretzki L, Mueller BM. Low-density-lipoprotein-receptor-related protein (LRP) interacts with a GTP-binding protein. Biochem J 1998;336:381–386.
12. Bacskai BJ, Xia MQ, Strickland DK, Rebeck GW, Hyman BT. The endocytic receptor protein LRP also mediates neuronal calcium signaling via N-methyl-D-aspartate receptors. Proc Natl Acad Sci USA 2000;97:11551–11556.

13. Zhuo M, Holtzman DM, Li Y, Osaka H, DeMaro J, Jacquin M, Bu G. Role of tissue plasminogen activator receptor LRP in hippocampal long-term potentiation. J Neurosci 2000;20:542–549.
14. Moestrup SK, Verroust PJ. Megalin-and cubilin- mediated endocytosis of protein-bound vitamins, lipids and hormones in polarized epithelia. Annu Rev Nutr 2001;21:407–428.
15. Willnow TE, Hilpert J, Armstrong SA, Rohlmann A, Hammer RE, Burns DK, Herz J. Defective forebrain development in mice lacking gp330/megalin. Proc Natl Acad Sci USA 1996;93:8460–8464.
16. McCarthy RA, Barth JL, Chintalapudi MR, Knaak C, Argraves WS. Megalin functions as an endocytic sonic hedgehog receptor. J Biol Chem 2002;277:25660–25667.
17. Brown MD, Banker GA, Hussaini IM, Gonias SL, Vandenberg SR. Low density lipoprotein receptor-related protein is expressed early and becomes restricted to a somatodendritic domain during neuronal differentiation in culture. Brain Res 1997;747:313–317.
18. Moestrup SK, Gliemann J, Pallesen G. Distribution of the alpha 2-macroglobulin receptor/low density lipoprotein receptor-related protein in human tissues. Cell Tissue Res 1992;269:375–382.
19. Rodriguez-Boulan E, Nelson WJ. Morphogenesis of the polarized epithelial cell phenotype. Science 1989;245:718–725.
20. Yeaman C, Grindstaff KK, Nelson WJ. New perspectives on mechanisms involved in generating epithelial cell polarity. Physiol Rev 1999;79:73–98.
21. Mostov KE, Verges M, Altschuler Y. Membrane traffic in polarized epithelial cells. Curr Opin Cell Biol 2000;12:483–490.
22. Lisanti MP, Siargiacomo M, Graeve L, Saltiel AR, Rodriguez-Boulan E. Polarized apical distribution of glycosyl-phosphatidylinositol anchored proteins in a renal cell epithelial line. Proc Natl Acad Sci USA 1988;85:9557–9561.
23. Lin S, Naim HY, Rodriguez AC, Roth MG. Mutations in the middle of the transmembrane domain reverse the polarity of transport of the influenza virus hemagglutinin in MDCK epithelial cells. J Cell Biol 1998;142:51–57.
24. Alfalah M, Jacob R, Naim HY. Intestinal dipeptidyl peptidase IV is efficiently sorted to the apical membrane through the concerted action of N- and O-glycans as well as association with lipid microdomains. J Biol Chem 2002;277:10683–10690.
25. Brown DA, Rose JK. Sorting of GPI-anchored proteins to glycolipid-enriched membrane subdomains during transport to the apical cell surface. Cell 1992;68:533–544.
26. Zurzolo C, van't Hof W, van Meer G, Rodriguez-Boulan E. VIP21/caveolin, glycosphingolipid clusters and the sorting of glycosylphosphatidylinositol-anchored proteins in epithelial cells. EMBO J 1994;13:42–53.
27. Rodriguez-Boulan E, Gonzalez A. Glycans in post-Golgi apical targeting: sorting signals or structural props? Trends Cell Biol 1999;9:291–294.
28. Marzolo MP, Bull P, Gonzalez A. Apical sorting of hepatitis B surface antigen (HBsAg) is independent of N-glycosylation and glycosylphosphatidylinositol-anchored protein segregation. Proc Natl Acad Sci USA 1997;94:1834–1839.
29. Chuang JZ, Sung CH. The cytoplasmic tail of rhodopsin acts as a novel apical sorting signal in polarized MDCK cells. J Cell Biol 1998;142:1245–1256.
30. Rotin D, Bar-Sagi D, Brodovich HO, Merilainen J, Lehto VP, Canessa CM, Rossier BC, Downey GP. An SH3 binding region in the epithelial Na+ channel (alpha rENaC) mediates its localization at the apical membrane. EMBO J 1994;13:4440–4450.
31. Moyer BD, Duhaime M, Shaw C, Denton J, Reynolds D, Karlson KH, Pfeiffer J, Wang S, Mickle JE, Milewski M, Cutting GR, Guggino WB, Li M, Stanton BA. The PDZ-interacting domain of cystic fibrosis transmembrane conductance regulator is required for functional expression in the apical plasma membrane. J Biol Chem 2000;275:27069–27074.
32. Dotti CG, Simons K. Polarized sorting of viral glycoproteins to the axon and dendrites of hippocampal neurons in culture. Cell 1990;62:63–72.
33. Pietrini G, Suh YJ, Edelmann L, Rudnick G, Caplan MJ. The axonal gamma-aminobutyric acid transporter GAT-1 is sorted to the apical membranes of polarized epithelial cells. J Biol Chem 1994;269:4668–4674.
34. Bradke F, Dotti CG. Membrane traffic in polarized neurons. Biochim Biophys Acta 1998;1404:245–258.
35. Ohno H, Tomemori T, Nakatsu F, Okazaki Y, Aguilar RC, Foelsch H, Mellman I, Saito T, Shirasawa T, Bonifacino JS. Mu1B, a novel adaptor medium chain expressed in polarized epithelial cells. FEBS Lett 1999;449:215–220.
36. Folsch H, Ohno H, Bonifacino JS, Mellman I. A novel clathrin adaptor complex mediates basolateral targeting in polarized epithelial cells. Cell 1999;99:189–198.
37. Matter K, Hunziker W, Mellman I. Basolateral sorting of LDL receptor in MDCK cells: the cytoplasmic domain contains two tyrosine-dependent targeting determinants. Cell 1992;71:741–753.
38. Hunziker W, Fumey C. A di-leucine motif mediates endocytosis and basolateral sorting of macrophage IgG Fc receptors in MDCK cells. EMBO J 1994;13:2963–2967.
39. Bello V, Goding JW, Greengrass V, Sali A, Dubljevic V, Lenoir C, Trugnan G, Maurice M. Characterization of a di-leucine-based signal in the cytoplasmic tail of the nucleotide-pyrophosphatase NPP1 that mediates basolateral targeting but not endocytosis. Mol Biol Cell 2001;12:3004–3015.
40. Lisanti MP, Tang ZL, Sargiacomo M. Caveolin forms a hetero-oligomeric protein complex that interacts with an apical GPI-linked protein: implications for the biogenesis of caveolae. J Cell Biol 1993;123:595–604.
41. Willnow TE, Goldstein JL, Orth K, Brown MS, Herz J. Low density lipoprotein receptor-related protein and gp330 bind similar ligands, including plasminogen activator-inhibitor complexes and lactoferrin, an inhibitor of chylomicron remnant clearance. J Biol Chem 1992;267:26172–26180.
42. Moestrup SK, Nielsen S, Andreasen P, Jorgensen KE, Nykjaer A, Roigaard H, Gliemann J, Christensen EI. Epithelial glycoprotein-330 mediates endocytosis of plasminogen activator-plasminogen activator inhibitor type-1 complexes. J Biol Chem 1993;268:16564–16570.
43. Stefansson S, Lawrence DA, Argraves WS. Plasminogen activator inhibitor-1 and vitronectin promote the cellular clearance of thrombin by low density lipoprotein receptor-related proteins 1 and 2. J Biol Chem 1996;271:8215–8220.
44. Willnow TE, Nykjaer A, Herz J. Lipoprotein receptors: new roles for ancient proteins. Nat Cell Biol 1999;1:E157–E162.
45. Nykjaer A, Dragun D, Walther D, Vorum H, Jacobsen C, Herz J, Melsen F, Christensen EI, Willnow TE. An endocytic pathway essential for renal uptake and activation of the steroid 25-(OH) vitamin D3. Cell 1999;96:507–515.
46. Willnow TE, Sheng Z, Ishibashi S, Herz J. Inhibition of hepatic chylomicron remnant uptake by gene transfer of a receptor antagonist. Science 1994;264:1471–1474.
47. Sousa MM, Norden AG, Jacobsen C, Willnow TE, Christensen EI, Thakker RV, Verroust PJ, Moestrup SK, Saraiva MJ. Evidence for the role of megalin in renal uptake of transthyretin. J Biol Chem 2000;275:38176–38181.
48. de Hoop MJ, Dotti CG. Membrane traffic in polarized neurons in culture. J Cell Sci 1993;17 (Suppl):85–92.
49. Hunziker W, Harter C, Matter K, Mellman I. Basolateral sorting in MDCK cells requires a distinct cytoplasmic domain determinant. Cell 1991;66:907–920.
50. Sugimoto H, Sugahara M, Folsch H, Koide Y, Nakatsu F, Tanaka N, Nishimura T, Furukawa M, Mullins C, Nakamura N, Mellman I, Ohno H. Differential recognition of tyrosine-based basolateral signals by AP-1B subunit μ1B in polarized epithelial cells. Mol Biol Cell 2002;13:2374–2382.

51. Gan Y, McGraw TE, Rodriguez-Boulan E. The epithelial-specific adaptor AP-1B mediates post-endocytic recycling to the basolateral membrane. Nat Cell Biol 2002;4:605–609.
52. Gokay KE, Young RS, Wilson JM. Cytoplasmic signals mediate apical early endosomal targeting of endotubin in MDCK cells. Traffic 2001;2:487–500.
53. Moyer BD, Denton J, Karlson KH, Reynolds D, Wang S, Mickle JE, Milewski M, Cutting GR, Guggino WB, Li M. A PDZ-interacting domain in CFTR is an apical membrane polarization signal. J Clin Invest 1999;104:1353–1361.
54. Harris MJ, Kuwano M, Webb M, Board PG. Identification of the apical membrane targeting signal of the multidrug resistance associated protein 2 (MRP2/cMOAt. J Biol Chem 2001;276:20876–20881.
55. Sun F, Hug MJ, Lewarchik CM, Yun CH, Bradbury NA, Frizzell RA. E3KARP mediates the association of ezrin and protein kinase A with the cystic fibrosis transmembrane conductance regulator in airway cells. J Biol Chem 2000;275:29539–29546.
56. Gotthardt M, Trommsdorff M, Nevitt MF, Shelton J, Richardson JA, Stockinger W, Nimpf J, Herz J. Interactions of the low density lipoprotein receptor gene family with cytosolic adaptor and scaffold proteins suggest diverse biological functions in cellular communication and signal transduction. J Biol Chem 2000;275:25616–25624.
57. Lou X, McQuistan T, Orlando R, Farquhar M. GAIP, GIPC and Gai3 are concentrated in endocytic compartments of proximal tubule cells: putative role in regulating megalin's function. J Am Soc Nephrol 2002;13:918–927.
58. Morelle W, Haslam SM, Ziak M, Roth J, Morris HR, Dell A. Characterization of the N-linked oligosaccharides of megalin (gp330) from rat kidney. Glycobiology 2000;10:295–304.
59. Arreaza G, Brown DA. Sorting and intracellular trafficking of a glycosylphosphatidylinositol-anchored protein and two hybrid transmembrane proteins with the same ectodomain in Madin-Darby canine kidney epithelial cells. J Biol Chem 1995;270:23641–23647.
60. Simons K, Ikonen E. Functional rafts in cell membranes. Nature 1997;387:569–572.
61. Zheng X, Lu D, Sadlers JE. Apical sorting of bovine enteropeptidase does not involve detergent-resistant association with sphingolipid-cholesterol rafts. J Biol Chem 1999;274:1596–1605.
62. Lipardi C, Nitsh L, Zurzolo C. Detergent-insoluble GPI-anchored proteins are apically sorted in Fisher rat thyroid cells, but interference with cholesterol or sphingolipids differentially affects detergent insolubility and apical sorting. Mol Biol Cell 2000;11:531–542.
63. Obermoeller LM, Chen Z, Schwartz AL, Bu G. Ca^{2+} and receptor-associated protein are independently required for proper folding and disulfide bond formation of the low density lipoprotein receptor-related protein. J Biol Chem 1998;273:22374–22381.
64. Li Y, Lu W, Marzolo MP, Bu G. Differential functions of members of the low density lipoprotein receptor family suggested by their distinct endocytosis rates. J Biol Chem 2001;276:18000–18006.
65. Bu G, Rennke S. Receptor-associated protein is a folding chaperone for low density lipoprotein receptor-related protein. J Biol Chem 1996;271:22218–22224.
66. Marmorstein AD, Zurzolo C, Le Bivic A, Rodriguez-Boulan E. Cell surface biotinylation techniques and determination of protein polarity. In: Celis JE, eds. Cell Biology: A Laboratory Handbook. San Diego: Academic Press; 1998. pp 341–350.
67. Matter K, Yamamoto EM, Mellman I. Structural requirements and sequence motifs for polarized sorting and endocytosis of LDL and Fc receptors in MDCK cells. J Cell Biol 1994;126: 991–1004.